

Co-evolution of black hole growth and star formation activity in local luminous infrared galaxies

A. Alonso-Herrero^{1,2}, M. Pereira-Santaella³, G. H. Rieke⁴, D. Rigopoulou⁵,
A. M. Diamond-Stanic⁶, A. Hernán-Caballero¹, and Y. Wang⁷

¹ Instituto de Física de Cantabria, CSIC-Universidad de Cantabria, 39005 Santander, Spain

² Augusto González Linares Senior Research Fellow

³ Istituto di Astrofisica e Planetologia Spaziali, INAF-IAPS, 00133 Rome, Italy

⁴ Steward Observatory, University of Arizona, Tucson, AZ 85721, USA

⁵ Astrophysics Department, University of Oxford, Oxford OX1 3RH, UK

⁶ CASS, University of California, San Diego, CA 92093, USA

⁷ National Astronomical Observatories, Chaoyang District, Beijing 100012, China

Abstract

We use *Spitzer* spectroscopic and imaging observations to study the co-evolution of black hole (BH) growth and star formation (SF) activity in a complete volume-limited sample of local Luminous Infrared Galaxies (LIRGs). Using a mid-infrared (mid-IR) spectral decomposition method we identify active galactic nuclei (AGN) with Seyfert-like luminosities and relatively small bolometric contributions (median $\sim 5\%$) in half of the LIRG nuclei. Combining mid-IR and AGN optical detections we obtain a 62% AGN detection rate in local LIRGs. We combine gas velocity dispersions of spectrally resolved [Ne III] $15.56\ \mu\text{m}$ and [O III] $\lambda 5007\text{\AA}$ lines and literature stellar velocity dispersions, and we obtain typical BH masses of $3 \times 10^7 M_{\odot}$ for local LIRGs. We find that the ratios of nuclear and integrated SF rates (SFR) to BH accretion rates are higher in local LIRGs than in optically selected Seyferts. We interpret our results in a scenario where local LIRGs with an AGN represent an early phase of the (possibly episodic) growth of BHs in massive spiral galaxies with high SFR, not necessarily associated with a major merger event.

1 Introduction

One of the most fundamental relations in extragalactic astronomy is that in the local universe the masses of supermassive black holes (BH, with masses $M_{\text{BH}} > 10^6 M_{\odot}$) correlate with the

stellar mass and velocity of the bulge of their host galaxies [29, 17, 30, 19]. This seems to imply that bulges and supermassive BH evolve together likely regulating each other. If sufficient matter becomes available in the very close vicinity of the BH to be accreted, then the nucleus of the galaxy will shine with enormous power as an active galactic nucleus (AGN, see [28]). Therefore, AGN activity is usually perceived as evidence of the presence of a supermassive BH at the center of its host galaxy.

By definition, luminous infrared (IR) galaxies (LIRGs) have $8 - 1000 \mu\text{m}$ luminosities in the range $L_{\text{IR}} = 10^{11} - 10^{12} L_{\odot}$. They are powered by both AGN and star formation (SF) activity and contain large amounts of molecular gas [40]. Their IR luminosities imply star formation rates (SFR) of between 17 and $170 M_{\odot} \text{yr}^{-1}$ using the [27] prescription, which assumes a Salpeter Initial Mass Function (IMF). If the same gas that is forming stars in the host galaxy reaches the gravitational potential of the BH (see [1] for a review on the different proposed mechanisms), then the gas will also feed the BH and an AGN phase will be triggered. Indeed, there is now observational evidence showing a relation between SF activity on sub-kiloparsec and bulge scales and the BH accretion rate (BHAR) in Seyfert galaxies [21, 15]. Numerical simulations also predict this relation on physical scales from pc to kpc, although with a lower significance for the integrated SFR of the galaxy (see [22]). Therefore, local LIRGs show propitious conditions to study the co-evolution of SFR activity and the BH growth as they show both high integrated and nuclear SFRs [2, 7] and a high occurrence of AGN and composite nuclei [46, 49, 6].

In this conference proceedings we study the co-evolution of the SF activity and the BH growth in the complete volume-limited sample of local LIRGs of [2, 6] using *Spitzer* imaging observations with the IRAC [16] and the MIPS [37] instruments, and spectroscopic observations with the IRS instrument [24]. We use these observations to identify AGN in the mid-infrared (mid-IR), to infer the AGN bolometric luminosities and BHAR, to estimate the nuclear ($\sim 1.5 \text{kpc}$) SFRs and compare them with the integrated values from the IR luminosities, and to infer the BH masses of those LIRGs hosting an AGN. Throughout this work we assume the following cosmology $H_0 = 70 \text{ km s}^{-1} \text{Mpc}^{-1}$, $\Omega_M = 0.3$ and $\Omega_{\Lambda} = 0.7$.

2 The sample and observations

For this work, we use the complete volume-limited sample of local LIRGs that was presented and discussed in detail by [2, 6]. Briefly, we drew the sample from the *IRAS* Revised Bright Galaxy Sample [42] to include all the sources with $\log(L_{\text{IR}}/L_{\odot}) \geq 11.05$ and $v_{\text{hel}} = 2750 - 5300 \text{ km s}^{-1}$. The sample is composed of 45 *IRAS* systems, with 8 containing multiple nuclei, that is, 53 individual galaxies. For the assumed cosmology the distances are in the range $\simeq 40 - 78 \text{ Mpc}$, with a median value of 65 Mpc. We calculated the IR ($8 - 1000 \mu\text{m}$) luminosities of the galaxies using the *IRAS* flux densities from [42]. For galaxies in groups and interacting galaxies not resolved by *IRAS* we assumed that the L_{IR} fraction of each component is proportional to the *Spitzer*/MIPS $24 \mu\text{m}$ flux density fraction. The IR luminosities of the individual galaxies are in the range $\log(L_{\text{IR}}/L_{\odot}) = 10.64 - 11.67$, with a median value of $\log(L_{\text{IR}}/L_{\odot}) = 11.12$. All the relevant information for the sample can be found in [6].

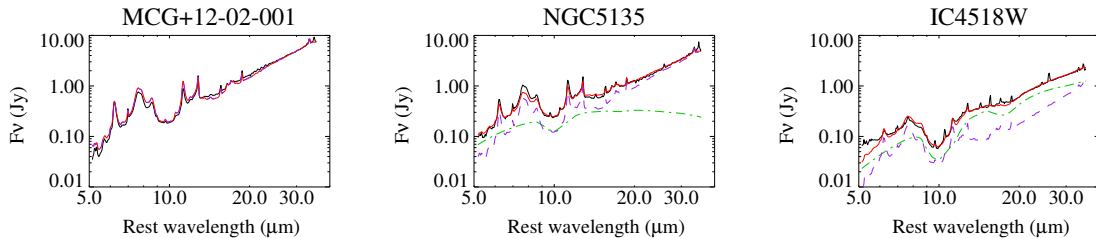


Figure 1: Examples of the AGN+SB decomposition method of the *Spitzer*/IRS SL+LL spectra for three local LIRGs with an increasing mid-IR AGN contribution from left to right. The black line is the observed spectrum in the rest-frame wavelength, the dashed-dotted (green) line is the fitted torus model, the dashed (purple) line is the scaled SB template, and the solid red line is the sum of the fitted SB and AGN components. Adapted from [6].

We obtained archival *Spitzer*/IRS $\sim 5 - 40 \mu\text{m}$ spectroscopy at low-resolution ($R \sim 60-120$) with the Short-Low (SL) and Long-Low (LL) modules and at high-resolution ($R \sim 600$) with the Short-High (SH) and Long-High (LH) modules. The observations of fifteen *IRAS* systems came from our own guaranteed time observation programs, and two more galaxies are from various programs. The rest of the IRS spectroscopy together with the IRAC and MIPS imaging data are part of The Great Observatories All-Sky LIRG Survey (GOALS) legacy program [8].

3 Results

3.1 AGN activity and AGN bolometric contribution

In this section, we use a spectral decomposition method to first identify AGN hosted in local LIRGS and second, if detected, to estimate the AGN bolometric contribution to the observed IR luminosity of the galaxies. To do so we performed a spectral decomposition of the *Spitzer*/IRS SL+LL $\sim 5 - 38 \mu\text{m}$ spectra into starburst (SB) and AGN components. The AGN emission in the mid-IR is assumed to be emission reprocessed by warm dust in the putative AGN dusty torus. We used the CLUMPY dusty torus models [33] together with the BAYESCLUMPY Bayesian routine [9] to fit the torus models to the data. For the SB component we used the average spectrum of local SBs of [10], as well as the LIRG templates of [38] in the range $\log(L_{\text{IR}}/L_{\odot}) = 10.5 - 12$.

Using the AGN+SB spectral decomposition we detected an AGN component in the mid-IR in 25 out of the 50 individual LIRG nuclei with IRS SL+LL spectroscopy. Figure 1 shows three examples of the mid-IR spectral decomposition: a galaxy without a mid-IR AGN detection (MCG +12-02-001), a galaxy with both AGN and SB contributions (NGC 5135) and a galaxy with an AGN dominated mid-IR spectrum (IC 4518W). We note that there are a few galaxies optically classified as composite (AGN/SB) or LINER for which we did not detect an AGN with our method. If we combine the optical and mid-IR AGN identifications, then the AGN detection rate is $\sim 62\%$ for the individual nuclei of local LIRGs and 75% for

IRAS systems. This is in good agreement with the AGN detection rate obtained from optical spectroscopy, if composite objects do indeed contain an AGN [49].

We find that on average the AGN contribution to the mid-IR continuum emission within the IRS SL+LL slits (typically covering the central ~ 4 kpc) of LIRGs is small, and decreases toward longer wavelengths. The median values range from 30% at $6 \mu\text{m}$ and $20 \mu\text{m}$ to 18% and 11% at $24 \mu\text{m}$ and $30 \mu\text{m}$, respectively. We used IRAC $5.8 \mu\text{m}$ and MIPS $24 \mu\text{m}$ images to derive the AGN contribution to the integrated galaxy emission at these mid-IR wavelengths. The median AGN contributions for those LIRGs with an AGN detection are 12% and 15% at $6 \mu\text{m}$ and $24 \mu\text{m}$, respectively, with only $\sim 6\%$ (3/50) of local LIRGs having a dominant ($> 50\%$) AGN contribution at $24 \mu\text{m}$.

One of the salient properties of the CLUMPY torus models is that the normalization needed to match them to the data scales directly with the AGN bolometric luminosity $L_{\text{bol}}(\text{AGN})$. Moreover, [5] recently showed that the values of $L_{\text{bol}}(\text{AGN})$ derived from the modeling of the nuclear IR emission of local Seyferts with the CLUMPY models agreed well with literature estimates. We derived AGN bolometric luminosities $L_{\text{bol}}(\text{AGN}) = (0.4 - 50) \times 10^{43} \text{ erg s}^{-1}$ with a median value of $L_{\text{bol}}(\text{AGN}) = 2 \times 10^{43} \text{ erg s}^{-1}$. That is, LIRGs host Seyfert-like AGN. These luminosities are in a fairly good agreement with those estimated from hard X-ray measurements after applying a bolometric correction [36].

The AGN bolometric contribution to the IR luminosity of the individual galaxies ranges between 1% and 70%, with an average value of $L_{\text{bol}}[\text{AGN}]/L_{\text{IR}} = 12\%$ (median of 5%) for those LIRGs with an AGN detection. For the AGN non-detections we estimate that if an AGN is present its bolometric contribution would be $L_{\text{bol}}[\text{AGN}]/L_{\text{IR}} < 1\%$. We conclude that, despite of the high AGN incidence in local LIRGs, the bulk of their IR luminosity is due to SF activity rather than AGN activity.

In Fig. 2, we compare the AGN bolometric contributions in local LIRGs with those of the local ultraluminous IR galaxies (ULIRGs) of [32]. In approximately one-third of local LIRGs the AGN bolometric contribution is mild, $L_{\text{bol}}[\text{AGN}]/L_{\text{IR}} \geq 0.05$. Only $\simeq 8\%$ of local LIRGs have a significant AGN contribution, $L_{\text{bol}}[\text{AGN}]/L_{\text{IR}} > 0.25$. It is also clear that the fraction of galaxies with $L_{\text{bol}}[\text{AGN}]/L_{\text{IR}} > 0.05$ increases at higher L_{IR} , going from 30% in local LIRGs to $\sim 50\%$ to ULIRGs with $L_{\text{IR}} < 3 \times 10^{12} L_{\odot}$. However, it is only at $L_{\text{IR}} > 5 \times 10^{12} L_{\odot}$ that the AGNs start dominating bolometrically the IR luminosity in a large fraction of local ULIRGs as shown by [32].

3.2 Black hole masses

The narrow line region (NLR) of AGN is sufficiently compact to be illuminated by the AGN, while large enough to feel the gravitational potential of the bulge. This is demonstrated by the relative good correlation between the gas and the stellar velocity dispersions of local AGN [18]. Thus, the velocity dispersion of the NLR ionized gas can be used to obtain an estimate of the BH mass in galaxies hosting an AGN. In the optical the $[\text{O III}]\lambda 5007$ emission line is widely used (see [18], and references therein), whereas in the mid-IR we can use the velocity dispersion of the fine structure lines $[\text{S IV}]10.51 \mu\text{m}$, $[\text{Ne III}]15.56 \mu\text{m}$, $[\text{Ne V}]14.32 \mu\text{m}$, and $[\text{O IV}]25.89 \mu\text{m}$, as demonstrated by [12].

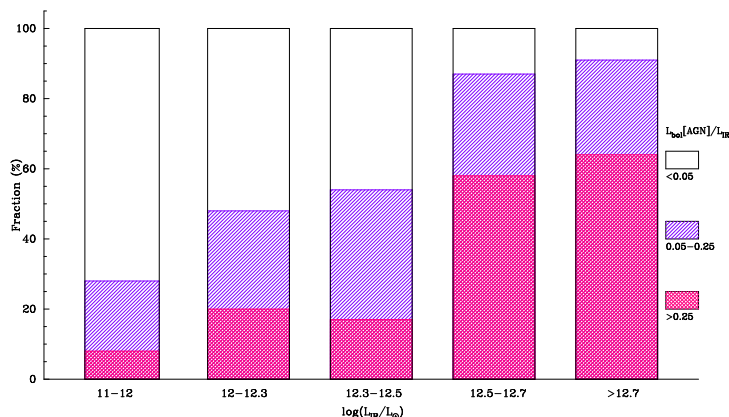


Figure 2: Fractional AGN bolometric contribution to the IR luminosity for the local sample of LIRGs compared with the local ULIRGs from [32]. We separated the AGN bolometric contributions $L_{\text{bol}}[\text{AGN}]/L_{\text{IR}}$ in three ranges: < 0.05 , $0.05 - 0.25$, > 0.25 . Adapted from [6].

In this work, we look for spectroscopically resolved [Ne III]15.56 μm lines in local LIRGs using the *Spitzer*/IRS SH spectroscopy. The [Ne III]15.56 μm flux and luminosity of local AGN are found to correlate well with those of the mid-IR [Ne v] lines at 14.3 and 24.3 μm (see [34, 12]). The high ionization potential of the [Ne v] lines indicates that they are mostly excited by AGN and thus the [Ne III]15.56 μm emission of AGN is likely to be as well. When compared with other mid-IR fine structure lines with relatively high ionization potentials (e.g., [S IV]10.51 μm , [O IV]25.89 μm , and the [Ne v] lines), the [Ne III]15.56 μm line is a good compromise between ionization potential, critical density, intensity of the line, and a clean region of the mid-IR spectrum for accurate measurements.

We detected spectrally resolved [Ne III]15.56 μm lines in $\sim 37\%$ of local LIRGs and measured gas velocity dispersions of between 70 and 368 km s^{-1} (corrected for instrumental resolution). We complemented these with our own analysis of the velocity dispersions of the core of the optical [O III] λ 5007 line of four LIRGs as well as with stellar velocity dispersion measurements from the literature. Figure 3 shows two examples of spectrally resolved [Ne III]15.56 μm and [O III] λ 5007 emission lines in our sample. Combining the gas and stellar velocity dispersions we obtained estimates of BH masses in the range $M_{\text{BH}} = 6 \times 10^6 M_{\odot}$ and $M_{\text{BH}} = 3.5 \times 10^8 M_{\odot}$, with a median value of $3 \times 10^7 M_{\odot}$. The majority of these estimates are for galaxies optically classified as Seyfert. The typical Eddington ratios ($L_{\text{bol}}(\text{AGN})/L_{\text{Edd}}$) for the LIRGs with an estimate of the BH mass are 2×10^{-2} , and are in the range $5 \times 10^{-4} - 0.1$. The lack of resolved [Ne III]15.56 μm lines at the *Spitzer*/IRS $R = 600$ resolution for most composite nuclei in our sample of local LIRGs would imply that they host less massive BH than those of the Seyfert LIRGs, that is, $M_{\text{BH}} < 2 - 3 \times 10^7 M_{\odot}$.

The BH masses of local LIRGs appear to be only marginally lower than those of local ULIRGs ($M_{\text{BH}} \sim 10^7 - 5 \times 10^8 M_{\odot}$, [45, 11]), while having similar stellar masses ($M_{\star} \sim 10^{11} M_{\odot}$). Local ULIRGs are also accreting with higher efficiencies (typical values of 0.08–0.4

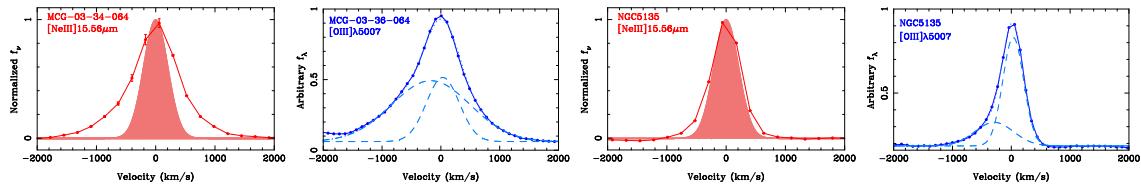


Figure 3: Observed profiles (solid lines and dots) of the spectrally resolved mid-IR [Ne III]15.56 μm (in red) and optical [O III] λ 5007 (in blue) lines for two LIRGs in our sample: MCG 03-34-064 (two left most) and NGC 5135 (two right most). Note that for these two galaxies the fitting of the optical line required two components (dashed lines, see [7] for more details). For the [Ne III]15.56 μm lines the shaded area represents the profile of an unresolved line at the IRS SH spectral resolution.

depending on the method used for estimating the BH mass, see [11, 47]) than LIRGs. In contrast, the moderately massive BH of local LIRGs appear to be more similar to those of the currently growing BH in the local universe hosted in late-type galaxies [21, 44].

3.3 Star formation activity

We computed the SFRs for our sample of LIRGs using a number of IR-based indicators, including the fine-structure [Ne II]12.81 μm line, the 11.3 μm polycyclic aromatic hydrocarbon (PAH) feature, and the total 8 – 1000 μm IR luminosity. For the integrated SFRs we made use of the IR luminosities of the individual galaxies after subtracting the AGN contribution and the [27] relation converted to a Kroupa IMF. We obtained total SFRs for the individual galaxies in the range 1–60 $M_{\odot} \text{ yr}^{-1}$. For the nuclear SFR we used the [Ne II]12.81 μm line and the 11.3 μm PAH feature measurements from the IRS SH module. At the median distance of 65 Mpc for our sample of LIRGs, the IRS SH slit width (4.7 arcsec) subtends typically 1.5 kpc. We used the recipes put forward by [15] for galaxies with IR luminosities below $10^{11} L_{\odot}$ using the [38] templates and a Kroupa IMF. We chose to use these calibrations rather than those for higher IR luminosities because the median value of the IR luminosity of the individual galaxies in our sample is $1.3 \times 10^{11} L_{\odot}$. In addition, the width of the IRS SH slit only probes the nuclear regions of our sample of LIRGs and thus lower IR luminosities. Finally, although it is not clear whether the presence of an AGN could destroy the PAH carriers or not, at the typical luminosities of the AGN hosted in local LIRGs the 11.3 μm PAHs do not seem to be affected [14].

In Fig. 4 (left panel), we compare the nuclear SFRs from the [Ne II]12.81 μm line and from the 11.3 μm PAH feature. In this figure we have color coded symbols by their AGN contribution to the IR luminosity of the galaxies (see Sect. 3.1). While the [Ne II]12.81 μm emission in low luminosity and moderate luminosity AGN is mostly produced by SF, in high luminosity AGN this emission line can also have an important contribution from the AGN [34]. As can be seen from this figure, the majority of LIRGs with small or no (<25%) AGN contribution show a good agreement between the derived nuclear SFRs using the two indicators. Indeed, we find that the ratio between the nuclear SFR estimated from the 11.3 μm PAH feature and that from the [Ne II]12.81 μm line is on average 1.0 ± 0.3 . In a few

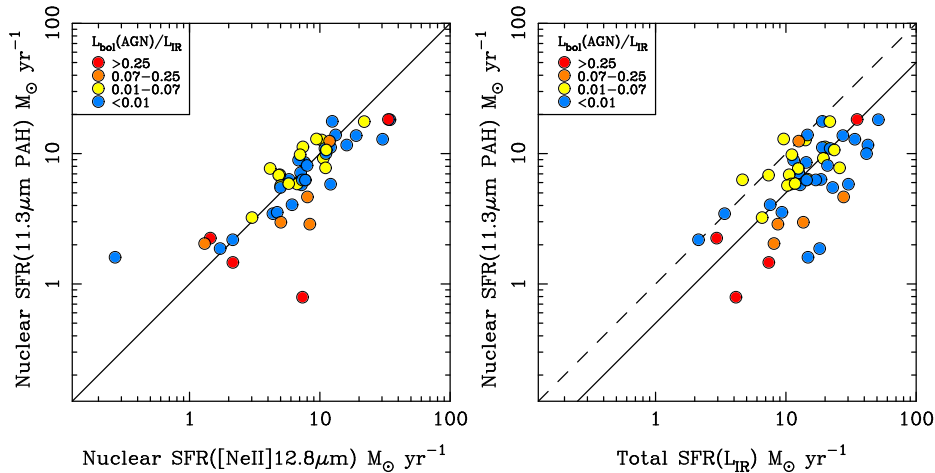


Figure 4: *Left panel:* nuclear SFRs from the $[\text{Ne II}]12.81 \mu\text{m}$ line vs. nuclear SFR from the $11.3 \mu\text{m}$ PAH feature. Colors denote the AGN bolometric contribution to L_{IR} of the individual galaxies: AGN fractions of $< 1\%$ or no contribution (blue), $1\% - 7\%$ (yellow), $7\% - 25\%$ (orange), and $> 25\%$ (red). The straight solid line is a 1:1 line and is the average value of the nuclear SFR calculated with the two estimators (see the text). *Right panel:* nuclear SFRs from the $11.3 \mu\text{m}$ PAH feature vs. integrated SFRs from L_{IR} after subtracting the AGN contribution. The straight solid line shows an average ratio between the nuclear and the total SFRs of 0.5 (see the text for details), which is typical of local LIRGs. The dashed line is a 1:1 relation for comparison.

cases with a high AGN contribution the nuclear SFR derived from the $[\text{Ne II}]12.81 \mu\text{m}$ line is higher than that from the $11.3 \mu\text{m}$ PAH feature, as expected if the AGN dominates the fine structure line emission. Given the good agreement between the nuclear SFR computed with the two methods and to avoid AGN contamination issues from now on for the nuclear SFR we use those derived from the $11.3 \mu\text{m}$ PAH feature. Thus, the individual nuclei of the sample of local LIRGs show values of the nuclear SFR of between ~ 0.8 and $\sim 20 M_{\odot} \text{yr}^{-1}$.

In Fig. 4 (right), we compare the total SFR against the nuclear (typically on scales of 1.5 kpc) SFR for the individual galaxies of the LIRG sample. As can be seen from this figure, a significant fraction of the individual galaxies in our sample have more than half of their total SFRs taking place outside the nuclear ($1 - 2 \text{ kpc}$) regions. We find that for the individual galaxies of the sample the average value of the nuclear SFR over the total SFR ratio is 0.5 ± 0.3 . This is in good agreement with findings of extended (over a few kpc) SF in local LIRGs using *Spitzer*/IRS spectral mapping [35], $\text{H}\alpha$ images [20, 3, 39], and *HST*/NICMOS narrow-band $\text{Pa}\alpha$ imaging [2]. We also note, however, that in $\sim 20\%$ of our volume-limited sample of LIRGs the nuclear emission accounts for most of the total SFR measured in the individual galaxies, as is the case for a large fraction of local ULIRGs.

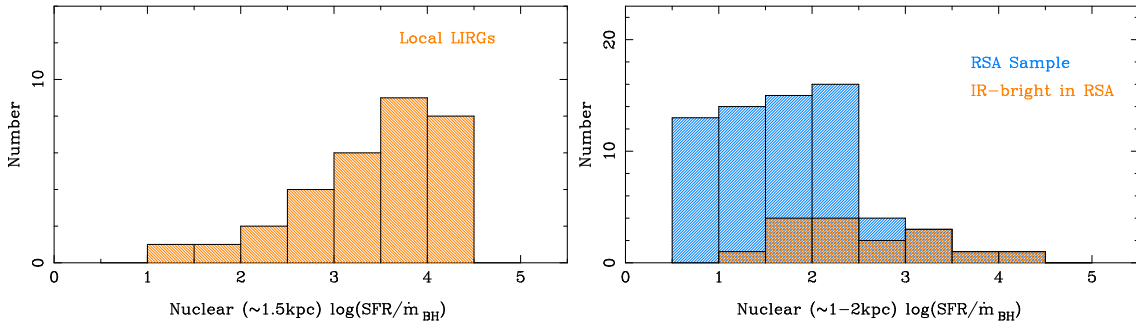


Figure 5: *Left panel:* distributions of the nuclear $\text{SFR}/\dot{m}_{\text{BH}}$ ratios for the local sample of LIRGs. *Right panel:* distribution of the nuclear $\text{SFR}/\dot{m}_{\text{BH}}$ ratios for the optically selected sample of RSA Seyfert galaxies (in blue, taken from [15]) only for AGN with $\dot{m}_{\text{BH}} > 10^{-4} M_{\odot} \text{yr}^{-1}$. In orange we mark those RSA Seyferts that are also IR-bright galaxies.

3.4 Relation between BH growth and star formation in local LIRGs

The presence of an AGN is an unambiguous signpost of a period of BH growth, as the AGN luminosity can be expressed as a function of the mass being accreted by the BH or BHAR (\dot{m}_{BH}) and the mass-energy conversion efficiency ϵ (see [1], and references therein). The distribution of the $\text{SFR}/\dot{m}_{\text{BH}}$ ratios can provide clues as to whether AGN and on-going SF activity are contemporaneous or not. Recent numerical simulations by [23] predict a time offset between the peaks of these activities, which is thought to depend on the physical scale within the galaxy and the dynamical time of the galaxy, among other parameters.

We used the typical value of $\epsilon = 0.1$ in the local universe [31] and the AGN bolometric luminosities estimated in Sect. 3.1, and obtained \dot{m}_{BH} of between 7×10^{-4} and $0.08 M_{\odot} \text{yr}^{-1}$ for local LIRGs. Figure 5 (left) shows the distribution of the SFR over the BHAR ratios for the sample of local LIRGs for the nuclear ($\sim 1.5 \text{kpc}$) regions. We have plotted in this figure the 25 LIRGs with estimates of the AGN bolometric luminosity from the mid-IR spectral decomposition. We also included galaxies with evidence of AGN activity but only an upper limit to their AGN luminosities and therefore, their $\text{SFR}/\dot{m}_{\text{BH}}$ ratios are lower limits. The nuclear ratios show a large spread in the values of $\text{SFR}(1.5\text{kpc})/\dot{m}_{\text{BH}}$ going from ~ 12 to 2×10^4 , with a median value of $\log(\text{SFR}(1.5\text{kpc})/\dot{m}_{\text{BH}}) = 3.5$.

Using only those LIRGs with an estimate of their AGN bolometric luminosities we find $\sum \text{SFR}/\sum \dot{m}_{\text{BH}} \simeq 3000$ (for the integrated SF), assuming that all LIRGs go through an AGN phase, that is, a $\sim 50\%$ duty cycle. The main uncertainty of this value comes from the estimates of the AGN bolometric luminosities (typically $\sim 0.4\text{dex}$, see [5, 6] for details). This ratio is a factor of a few higher than the local normalization of the BH mass vs. bulge mass relation [30, 19] and the observed ratio of the local population of bulge-dominated galaxies ($\sim 10^3$, see [21]). This result is explained because LIRGs (and ULIRGs) are probing the high end of the SF distribution in the local universe. The observed ratio for LIRGs is, however similar to that of local bulge galaxies during the first $0.2 - 0.3 \text{Gyr}$ of the starburst [48].

The median value of $\text{SFR}(1.5\text{kpc})/\dot{m}_{\text{BH}}$ for the sample of local LIRGs is considerably

higher than that of the local Seyferts in the revised-Shapley-Ames catalog (RSA), as can be seen from the right panel of Fig. 5 (data from [15]). Of course, this is not completely unexpected since local LIRGs, including those hosting an AGN, are basically selected by their SF activity (Sect. 3.1), whereas the RSA Seyferts are selected by their host galaxy magnitudes (i.e., approximately stellar mass).

There exists a good correlation between the nuclear ($r = 1$ kpc) SFR and the BHAR for the RSA Seyfert galaxies of the form $\text{SFR} \propto \dot{m}_{\text{BH}}^{0.6}$, with a scatter of 0.5dex (see [15] for more details). A similar relation is also predicted by the numerical simulations of [22]. However, a large fraction of the RSA Seyferts classified as IR-bright (that is, with $\log(L_{\text{IR}}/L_{\odot}) > 10.8$) lie above this relation. In other words, they tend to show an excess of nuclear SFR for their measured BHAR when compared to Seyfert galaxies (see [7] for more details). Given the fact that the AGN in the RSA sample are not very different from those in local LIRGs, this result implies that the IR-active star forming phase comes first and *the dormant AGN does not know about it*. Any increased AGN activity would come later. Such delays between the onset of the SF activity and the BH growth are also observed in other local Seyfert galaxies and bulge galaxies (e.g., [13, 48]). This would also agree with the prediction that once there is sufficient fuel to grow the BH at the (or near the) Eddington limit, having a large supply of gas at large radii does not increase the BHAR [23].

4 Discussion and summary

Major mergers do not dominate in numbers the population of local LIRGs, especially at $L_{\text{IR}} < 3 \times 10^{11} L_{\odot}$ [41, 2, 26, 3]. This probably indicates that in most LIRGs the BH growth (at least the current episode) has been taking place in a less *violent* fashion, e.g., via minor mergers, fly-by companions, and/or secular processes. The triggering of the activity in local ULIRGs (and perhaps the most luminous local LIRGs), in contrast, is driven by major mergers and in consequence ULIRGs tend to host more luminous AGN than those of local LIRGs (Sects. 3.1 and 3.2) and marginally more massive BH. The stellar populations of non-major merger LIRGs are mostly accounted for in mass by an evolved stellar population formed a few Gyr ago plus a much smaller contribution in mass from a relatively young stellar population. The latter formed in a period of SF that started about 0.5 – 1 Gyr ago [26, 4]. Given the high SFR of local LIRGs, this last period of SF is still active at present. On the other hand, the minority of major merger LIRGs in the local universe show evidence of a more recent period of SF that consumed the gas faster, that is, they experienced a more *bursty* SFR. [26] also found that Seyfert activity in most local LIRGs appears a few hundred million years after the onset of the current period of SF. Therefore, we assume that the composite (AGN/SB) phase occurred prior to the Seyfert phase when the SFR decreases and a new BH growth episode begins.

The cartoon in Fig. 6 illustrates our proposed scenario for the *current* BH growth in a non-merger local LIRG. The galaxy has an old stellar population formed a few Gyr ago [26, 4] and started the current period of SF less than 1 Gyr ago. Because the galaxy did not experience a major merger but rather a less *violent* process that induced the last episode of SF, we can assume an exponentially SFR where $\text{SFR}(t) = \text{SFR}_0 e^{-t/\tau}$ and τ is the e-folding

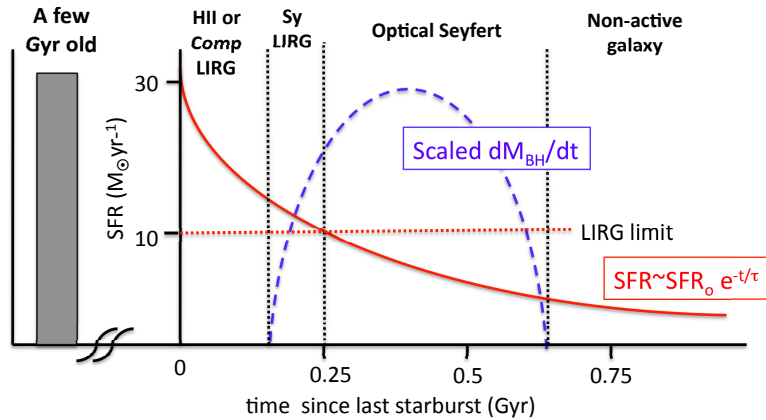


Figure 6: Cartoon (not drawn to scale) depicting the proposed scenario for the evolution of a local non-major merger LIRG. The last episode of SF is assumed to be an exponentially decaying SFR (red curve) with an e-folding time τ . The current period of BH growth is assumed to have a 5×10^8 yr lifetime (blue curve). The BHAR would be on average ~ 3000 times lower than the SFR during the LIRG phase.

time. From the position of local AGN on the color-magnitude diagram, [43] demonstrated that the e-folding time cannot be too short ($\tau \sim 10$ Myr or bursty) or too long (i.e., constant SFR). The high AGN detection rate in local LIRGs (see Sect. 3.1) implies that LIRGs are able to feed the BH (i.e., show AGN activity) during half of the LIRG-phase (defined as having integrated $\text{SFR} > 10 \text{ M}_\odot \text{ yr}^{-1}$, see Fig. 4). Moreover, given the moderate BH masses inferred for LIRGs (Sect. 3.2), this AGN activity is likely to be sustained for $\sim 5 \times 10^8$ yr, which is the typical lifetime of the BH growth for $M_{\text{BH}} < 10^8 \text{ M}_\odot$ (see [31]).

In this simple scenario, the galaxy would be first classified optically as an H II LIRG and would show elevated integrated and nuclear SFRs. After a time, provided that the gas reaches the BH gravitational potential, the existing BH starts accreting material at a sufficiently high rate. Then the galaxy would have a Seyfert-like AGN luminosity. Because there is still an elevated nuclear SFR, the galaxy would be optically classified as composite (AGN/SB) and later as a Seyfert LIRG as the SFR decreases. In both cases the $\text{SFR}/\dot{m}_{\text{BH}}$ ratios would be on average higher than those of the majority of optically identified Seyferts (Sect. 3.4 and Fig. 5). After a few hundred million years the SFR is below $10 \text{ M}_\odot \text{ yr}^{-1}$ and thus the galaxy would not be classified as a LIRG any longer. However, the AGN phase may still be active for a time as Seyfert-like AGNs do not require large amounts of gas to remain active (see [23]). The galaxy would be then identified as an optical Seyfert with a lower value of the $\text{SFR}/\dot{m}_{\text{BH}}$ ratio and a moderate SFR. The latter is observed in the local universe where AGN tend to live in hosts with enhanced SF activity when compared to non-active galaxies of similar stellar masses [25]. Eventually the BH accretion rate would be so low that the galaxy may not be identified as a Seyfert. In this scenario the delay between the onset of the SF activity and the peak of the BH accretion rate would be a few hundred million years from an integrated point of view, consistent with the predictions of [23].

In summary, local LIRGs with an AGN represent an early phase of the (possibly episodic) growth of BHs in massive spiral galaxies with high SFR, not necessarily associated with a major merger event. An H II LIRG phase would predate the AGN LIRG phase. The latter in turn would be followed by an optically identified AGN phase where the galaxy still shows an appreciable SFR but below the LIRG limit. Although the triggering mechanisms for the SB and AGN activity of LIRGs and ULIRGs might be different, it appears that the sequence of events is similar. Namely, ULIRGs and the most luminous LIRGs are believed to involve the interaction between two gas-rich galaxies that results first in a high SFR and then an optical QSO phase (see, e.g., [40, 49]). The end product, in contrast, is rather different with ULIRGs probably evolving into classical ellipticals and LIRGs remaining late-type galaxies.

Acknowledgments

A.A.-H. and M.P.-S. acknowledge support from the Spanish Plan Nacional de Astronomía y Astrofísica under grant AYA2009-05705-E. A.A.-H. and A.H.-C. are also funded by the Universidad de Cantabria through the Augusto González Linares Program. This work is based on observations made with the Spitzer Space Telescope, which is operated by the Jet Propulsion Laboratory, California Institute of Technology under NASA contract 1407. M.P.-S. is funded by an ASI fellowship under contract I/005/11/0.

References

- [1] Alexander, D. M. & Hickox, R. C. 2012, *NewAR*, 56, 93
- [2] Alonso-Herrero, A., et al. 2006, *ApJ*, 650, 835
- [3] Alonso-Herrero, A., et al. 2009, *A&A*, 506, 1541
- [4] Alonso-Herrero, A., et al. 2010, *A&A*, 522, A7
- [5] Alonso-Herrero, A., Ramos Almeida, C., Mason, R., et al. 2011, *ApJ*, 736, 82
- [6] Alonso-Herrero, A., Pereira-Santaella, M., Rieke, G. H., & Rigopoulou, D. 2012, *ApJ*, 744, 2
- [7] Alonso-Herrero, A., et al. 2013, *ApJ*, 765, 78
- [8] Armus, L., et al. 2009, *PASP*, 121, 559
- [9] Asensio Ramos, A. & Ramos Almeida, C. 2009, *ApJ*, 696, 2075
- [10] Brandl, B., et al. 2006, *ApJ*, 653, 1129
- [11] Dasyra, K. M., et al. 2006, *ApJ*, 651, 835
- [12] Dasyra, K. M., et al. 2011, *ApJ*, 740, 94
- [13] Davies, R. I., et al. 2007, *ApJ*, 671, 1388
- [14] Diamond-Stanic, A. M., & Rieke, G. H. 2010, *ApJ*, 724, 140
- [15] Diamond-Stanic, A. M., & Rieke, G. H. 2012, *ApJ*, 746, 168
- [16] Fazio, G. G., et al. 2004, *ApJS*, 154, 10

- [17] Gebhardt, K., et al. 2000, ApJ, 543, L5
- [18] Greene, J. E. & Ho, L. C. 2005, ApJ, 627, 721
- [19] Häring, N., & Rix, H. W. 2004, ApJ, 604, L89
- [20] Hattori, T., et al. 2004, AJ, 127, 736
- [21] Heckman, T. M., et al. 2004, ApJ, 613, 109
- [22] Hopkins, P. F. & Quataert, E. 2010, MNRAS, 407, 1529
- [23] Hopkins, P. F. 2012, MNRAS, 420, L8
- [24] Houck, J. R., et al. 2004, ApJS, 154, 18
- [25] Kauffmann, G., et al. 2003, MNRAS, 346, 1055
- [26] Kaviraj, S. 2009, MNRAS, 394, 1167
- [27] Kennicutt, R. C. Jr. 1998, ARA&A, 36, 189
- [28] Lynden-Bell, D. 1969, Nature, 223, 690
- [29] Magorrian, J., et al. 1998, AJ, 115, 2285
- [30] Marconi, A. & Hunt, L. K. 2003, ApJ, 589, L21
- [31] Marconi, A., et al. 2004, MNRAS, 351, 169
- [32] Nardini, E., Risaliti, G., Watabe, Y., Salvati, M., & Sani, E. 2010, MNRAS, 405, 2505
- [33] Nenkova, M., Sirocky, M. M., Nikkuta, R., Ivezić, Z., & Elitzur, M. 2008, ApJ, 685, 160
- [34] Pereira-Santaella, M., et al. 2010, ApJ, 725, 2270
- [35] Pereira-Santaella, M., et al. 2010, ApJS, 188, 447
- [36] Pereira-Santaella, M., et al. 2011, A&A, 535, A93
- [37] Rieke, G. H., et al. 2004, ApJS, 154, 25
- [38] Rieke, G. H., et al. 2009, ApJ, 692, 556
- [39] Rodríguez-Zaurín, J., et al. 2011, A&A, 527, 60
- [40] Sanders, D.B. & Mirabel, F. I. 1996, ARA&A, 34, 749
- [41] Sanders, D.B. & Ishida C., 2004, ASP Conf. Ser., 210, 230
- [42] Sanders, D. B., Mazzarella, J. M., Kim, D.-C., Surace, J. A., & Soifer, B. T. 2003, AJ, 126, 1607
- [43] Schawinski, K., et al. 2009, ApJ, 692, L19
- [44] Schawinski, K., et al. 2010, ApJ, 711, 284
- [45] Tacconi, L. J., et al. 2002, ApJ, 580, 73
- [46] Veilleux, S., et al. 1995, ApJS, 98, 171
- [47] Veilleux, S., et al. 2009, ApJS, 182, 628
- [48] Wild, V., Heckman, T., & Charlot, S. 2010, MNRAS, 405, 933
- [49] Yuan, T.-T., Kewley, L. J., & Sanders, D. B. 2010, ApJ, 709, 884